PHYSICAL REVIEW A VOLUME 22, NUMBER 1 JULY 1980

Electron-impact ionization cross sections for highly ionized hydrogen- and lithium-like atoms

S. M. Younger
National Bureau of Standards, Washington D.C. 20234
(Received 3 March 1980)

Electron-impact ionization cross sections for highly ionized atoms in the hydrogen and lithium isoelectronic sequences have been computed in several variants of the Coulomb-Born and distorted-wave approximations. Electron exchange in the transition matrix element and Coulomb distortion of the partial waves were found to be important. The results are compared to recent crossed-beam experimental data and to other theoretical predictions.

I. INTRODUCTION

There is currently an urgent need within the fusion plasma community for accurate electron-impact ionization cross sections for use in modeling ionization balance in high-temperature plasmas as well as for certain diagnostic applications.[1] There exist very few determinations of such data, however, either experimental or theoretical, for the highly ionized species encountered in large plasma machines.[2,3] Those results which are available are often not complete enough to allow the isoelectronic scaling of the cross section to be determined.

This paper describes calculations of electron-impact ionization cross sections for highly ionized atoms in the hydrogen and lithium isoelectronic sequences, using several variants of the Coulomb-Born and distorted-wave approximations. Explicit attention is given the isoelectronic behavior of the cross section, in an attempt to identify scaling laws useful in the extrapolation and interpolation of existing data. The results are compared to recent crossed-beam experimental data, as well as to other theoretical studies and the semiempirical method of Lotz.[4] Isoelectronic plots of the distorted-wave results are given which allow interpolation of nonrelativistic cross sections throughout the hydrogen and lithium isoelectronic sequences.

II. THEORY

A. General

The electron-impact ionization cross section Q may be written (in units of πa_0^2, where $a_0 = 0.529 \times 10^{-8}$ cm is the Bohr radius) as[5]

$$Q = \int_0^{E/2} \sigma(\epsilon, E_i)\, d\epsilon \,, \tag{1}$$

where E_i is the incident electron energy, $E = E_i - I$, I is the ionization energy, and ϵ is the energy of the ejected electron. All energies are in rydbergs. The ejected electron is defined as the final-state electron with the lower energy, the scattered electron as the one with the higher energy. The differential cross section $\sigma(\epsilon, E_i)$ is given by

$$\sigma(\epsilon, E_i) = \frac{16}{\pi E_i} \sum_{l_i l_e l_f} (2L+1) I_{l_i l_e l_f}(\epsilon, E_i) \,, \tag{2}$$

where l_i, l_e, and l_f are the orbital angular momenta of the incident, ejected, and scattered electrons, respectively, L is the conserved total angular momenta of the atom plus electron system, and

$$\begin{aligned} I_{l_i l_e l_f} L &= |f|^2 + |g|^2 - \alpha |f|\,|g| \\ &\equiv \sigma_d + \sigma_e - \sigma_{\text{int}} \,. \end{aligned} \tag{3}$$

The direct and exchange scattering amplitudes f and g for ionization of a single electron are

$$f = \sum_{\lambda=0} f_\lambda(l_b l_i l_e l_f L) \left(P_b P_i \left| \frac{1}{r_{12}} \right| P_e P_f \right)_\lambda \,, \tag{4}$$

$$g = \sum_{\lambda=0} f_\lambda(l_b l_i l_f l_e L) \left(P_b P_i \left| \frac{1}{r_{12}} \right| P_f P_e \right)_\lambda \,, \tag{5}$$

and α is a phase factor. l_b is the orbital angular momentum of the target electron. r_{12} is the relative separation of electrons 1 and 2. P_b, P_i, P_e, and P_f are the radial orbitals corresponding to the bound, initial-scattering, ejected, and final-scattering states, respectively. The angular factor $f_\lambda(l_a l_b l_c l_d L)$ is

$$f_\lambda(l_a l_b l_c l_d L) = (-1)^{l_a + l_c - L} [(2l_a+1)(2l_b+1)(2l_c+1)(2l_d+1)]^{1/2} \times \begin{pmatrix} l_a & l_c & \lambda \\ 0 & 0 & 0 \end{pmatrix} \begin{pmatrix} l_b & l_d & \lambda \\ 0 & 0 & 0 \end{pmatrix} \begin{Bmatrix} l_a & l_b & L \\ l_d & l_c & \lambda \end{Bmatrix} \,. \tag{6}$$

TABLE I. Definitions of partial-wave potentials used for ionization cross-section calculations.

Potential	Hydrogen-like	Lithium-like
V_{CB}	$-\frac{Z-1}{r}$	$-\frac{Z-3}{r}$
V_{DW_1}	$-\frac{Z}{r}+J_{1s}(r)$ [a]	$-\frac{Z}{r}+2J_{1s}(r)+J_{2s}(r)$
V_{DW_2}	$-\frac{Z}{r}$	$-\frac{Z}{r}+2J_{1s}(r)$

[a] $J_{ns}(r)=\frac{1}{r}\int_0^r P_{ns}^2(\rho)d\rho+\int_r^\infty \frac{P_{ns}^2(\rho)}{\rho}d\rho$.

The round brackets in Eqs. (4) and (5) denote radial integrations:

$$\left(P_aP_b\left|\frac{1}{r^{12}}\right|P_cP_d\right)_\lambda=\int_0^\infty dr_1\int_0^\infty dr_2P_aP_b\left(\frac{r_<^\lambda}{r_>^{\lambda+1}}\right)P_cP_d \tag{7}$$

with $r_>(r_<)$ the greater (smaller) of r_1 and r_2.

Partial-wave continuum states were generated numerically over a 350-point radial grid. Matrix elements were calculated using Simpson's rule. The maximum values of l_i, l_e, and l_f were 12, 7, and 12, respectively, and the energy integral in Eq. (1) was approximated by a three-point Gauss-Legendre formula. For the lithium-like ions, Hartree-Fock target states and empirical ionization energies were employed. Careful attention was given the partial cross section summations to be sure that adequate convergence was obtained in all cases.

B. Approximation schemes for the ionization cross section

Within the general framework of Eqs. (1)–(3), it is possible to define a variety of approximations for the ionization cross section depending on the choice of target wave function, partial wave potentials, and the phase of the interaction term σ_{int}. All of the cross sections given here were computed in the so-called "maximum interference" approximation[5] with $\alpha=1$. Table I gives definitions of the potentials used in the present study. The partial waves are solutions of the radial Schrödinger equation

$$\left(\frac{d}{dr^2}+\frac{l(l+1)}{r^2}-2V(r)\right)P_{\epsilon l}(r)=\epsilon P_{\epsilon l}(r), \tag{8}$$

where $V(r)$ is one of the potentials in Table I, and $\epsilon=k^2$ is the partial-wave energy in rydbergs. An approximation is thus defined in terms of the partial waves occurring in the direct and exchange scattering amplitudes (see Table II).

Approximations CBT (Coulomb-Born truncated) and DWT (distorted-wave truncated) omit exchange and interference entirely. Approximations CBE and DWE recompute the partial waves occurring in the final state of the exchange scattering amplitude to ensure that overlaps in the matrix element only occur between orthogonal functions computed in the same potential. The plane-wave Born (PWB) approximation uses plane-wave (spherical Bessel functions) partial waves and neglects exchange and interference effects. Note in the lithium sequence that the final-state orbital overlapping the initial bound orbital is always computed in the static potential of the nucleus and the $1s^2$ core. Thus in the lithium sequence "Coulomb-Born" and "plane-wave Born" apply to the scattered waves.

None of the present approximations account for resonances associated with compound states of the electron plus atom system. The inclusion of such effects would be a formidable task considering the triple partial-wave expansion occurring in the ionization matrix element. The agreement of nonresonance calculations with experiment[2] suggests that the omission of such complex processes may not be serious.

For lithium-like ions in the energy range considered here there is no contribution from either direct ionization of the $1s^2$ core or from excitation of core-excited states which later autoionize. Simple considerations based on the asymptotic $Z=\infty$

TABLE II. Approximations for the electron-impact ionization cross section in terms of the partial waves occurring in the direct and exchange matrix element and the phase of the interference term.

Approximation	Direct matrix element V_i	V_e	V_f	Exchange matrix element V_i	V_e	V_f	σ_{int}
CBT	CB_1	DW_2	CB_1				omit
DWT	DW_1	DW_2	DW_1				omit
CBE	CB_1	DW_2	CB_1	CB_1	CB_1	DW_2	σ_{int}^{max}
DWE	DW_1	DW_2	DW_1	DW_1	DW_1	DW_2	σ_{int}^{max}

TABLE III. Scaled electron-impact ionization cross sections uI^2Q for highly ionized hydrogen-like atoms in units of πa_0^2 (Ry)^2.

Ion	u	DWE [a]	DWT [a]	CBE [a]	CBT [a]	PWB [b]
He II	1.125	0.230	0.246	0.241	0.243	0.104
I=4 Ry	1.25	0.405	0.460	0.457	0.490	0.278
	1.50	0.795	0.948	0.856	0.980	0.697
	2.25	1.83	2.24	1.87	2.25	1.98
C VI	1.125	0.273	0.278	0.273	0.280	0.104
I=36 Ry	1.25	0.520	0.551	0.521	0.554	0.278
	1.50	0.964	1.07	0.962	1.07	0.697
	2.25	2.03	2.36	2.02	2.36	1.98
Ne X	1.125	0.288	0.286	0.287	0.287	0.104
I=100 Ry	1.25	0.546	0.565	0.544	0.566	0.278
	1.50	1.00	1.09	1.00	1.09	0.697
	2.25	2.08	2.38	2.07	2.38	1.98
$Z=\infty$	1.125			0.318	0.297	0.104
	1.25			0.599	0.584	0.278
	1.50			1.09	1.12	0.697
	2.25			2.20	2.41	1.98

[a] See Table II for an explanation of approximation labels.
[b] Plane-wave Born. Scaling with Z results in the same uI^2Q for each ion.

ion show that direct 1s ionization does not occur until $u_{2s} > 4$, while excitation-autoionization is restricted to the region $u_{2s} > 3$. For ions with finite charge such processes should occur at even higher u_{2s}.

III. RESULTS

Table III contains the results of calculations of electron-impact ionization cross sections for He II, C VI, and Ne X following the procedures outlined in the previous section. To eliminate the gross energy and charge-state dependence of the cross section, we tabulate the quantity uI^2Q, where u is the energy in threshold units, and I is the ionization energy in rydbergs. Figure 1 is a Fano plot of the plane-wave Born, Coulomb-Born, and distorted-wave approximation cross sections for He II compared to the experimental crossed-beam data of Peart *et al.*[6] The DWE and CBE theoretical curves are both in good agreement with experiment. Similar data for the lithium-like ions Be II, O VI, and Mg X are given in Table IV. Figure 2 is a Fano plot of the scaled cross sections for O VI along with the crossed-beam data of Crandall *et al.*,[7] the CBE data of Jakubowica and Moores,[8] and the scaled CBE results of Golden and Sampson.[9]

In Figs. 3 and 4 we present isoelectronic plots of the DWE ionization cross sections uI^2Q for the hydrogen and lithium sequences. Each curve corresponds to a fixed incident energy in threshold units $u = E_i/I$. The y intercepts of these curves correspond to $Z = \infty$. Ioselectronic plots such as these are particularly useful in that they allow interpolation of the ionization cross section for any ion in the hydrogen and lithium isoelectronic sequences within the specified energy range. Figures 5 and 6 compare the cross sections for C IV

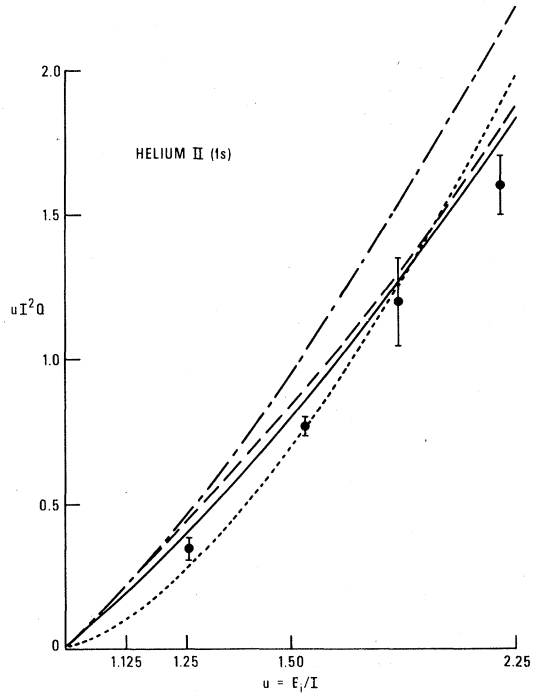

FIG. 1. Fano plot of the scaled electron-impact ionization cross section uI^2Q for He II (1s) in units of πa_0^2 (Ry)^2. -·-·-DWT; ——— DWE; ---CBE; -----plane-wave Born; ● crossed-beam experiment, Ref. 6.

TABLE IV. Scaled electron-impact ionization cross sections uI^2Q for highly ionized lithium-like atoms in units of πa_0^2 (Ry)^2.

	u	DWE[a]	DWT[a]	CBE[a]	CBT[a]	PWB[b]
Be II	1.125	0.269	0.237	0.310	0.234	0.145
I=1.339 Ry	1.25	0.493	0.467	0.564	0.462	0.334
	1.50	0.866	0.903	0.973	0.891	0.752
	2.25	1.67	1.94	1.80	1.92	1.79
O VI	1.125	0.290	0.277	0.284	0.278	0.135
I=10.156 Ry	1.25	0.538	0.541	0.529	0.542	0.330
	1.50	0.953	1.02	0.943	1.02	0.751
	2.25	1.84	2.13	1.83	2.13	1.81
Mg X	1.125	0.312	0.292	0.309	0.292	0.136
I=27.024 Ry	1.25	0.578	0.567	0.572	0.568	0.335
	1.50	1.02	1.07	1.01	1.07	0.757
	2.25	1.92	2.19	1.91	2.19	1.83
$Z=\infty$	1.125			0.353	0.316	0.171
	1.25			0.649	0.611	0.338
	1.50			1.13	1.13	0.764
	2.25			2.07	2.32	1.85

[a] See Table II for an explanation of approximation labels.
[b] Plane-wave Born.

and N V interpolated from these graphs to the experimental data of Crandall *et al.*[7] as well as the Coulomb-Born calculations of Jakubowicz and Moores[8] and Golden and Sampson.[9] Excellent agreement between theory and experiment is obtained for N V, but all theoretical predictions lie above the measured points for C IV. Such a discrepancy between data for adjacent ions is puzzling in light of the smooth isoelectronic behavior of the scaled cross section apparent from Figs. 3 and 4.

The semiempirical formula of Lotz[4] for the ionization cross section appears as a horizontal line on an isoelectronic plot. Figs. 3 and 4 show agree agreement to within about 30% between this simple fit and DWE calculations, the larger deviations being for high energies and low charge states.

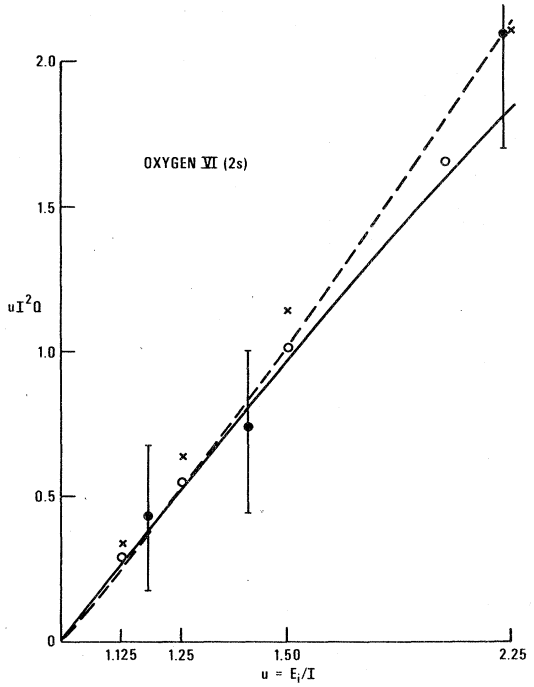

FIG. 2. Fano plot of the scaled electron-impact ionization cross section uI^2Q for O VI (2s) in units of πa_0^2 (Ry)^2. --- DWT (present); —— DWE (present); • crossed-beam experiment, Ref. 7; ○ Coulomb-Born exchange, Ref. 8; × Coulomb-Born exchange scaled from $Z=\infty$ data, Ref. 9.

IV. DISCUSSION

Equations 4 and 5 for the direct and exchange scattering amplitudes assume orthogonality be-

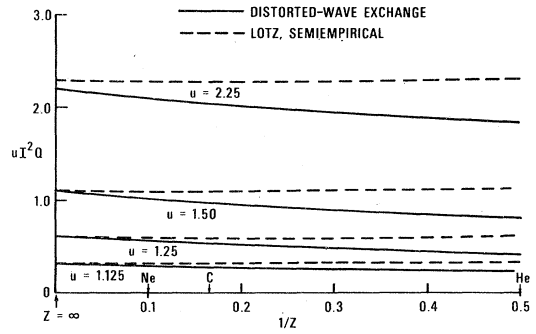

FIG. 3. Isoelectronic plot of the scaled electron-impact ionization cross section uI^2Q for ionization from the ground state of hydrogen-like ions. The units of uI^2Q are πa_0^2 (Ry)^2. —— DWE (present); ---semiempirical formula of Lotz, Ref. 4.

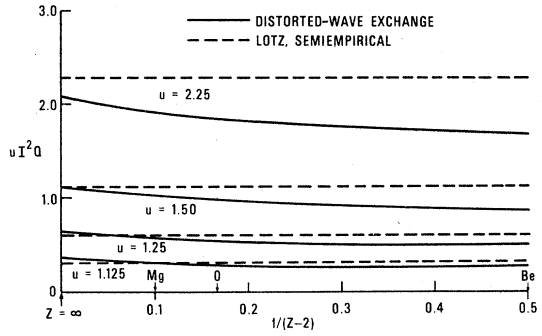

FIG. 4. Isoelectronic plot of the scaled electron-impact ionization cross section uI^2Q for ionization of the $2s\,^2S$ ground-state of lithium-like ions. The units of uI^2Q are πa_0^2 (Ry)^2. —— DWE (present); ---semiempirical formula of Lotz, Ref. 4.

tween overlapping initial- and final-state radial orbitals. While this is always true within the Born-exchange (BE) approximation for hydrogen-like ions, the use of a Hartree-Fock target function and static potential distorted ejected waves for lithium-like ions could introduce nontrivial monopole terms into the $\lambda = 0$ radial matrix elements. To test the sensitivity of the total cross section to

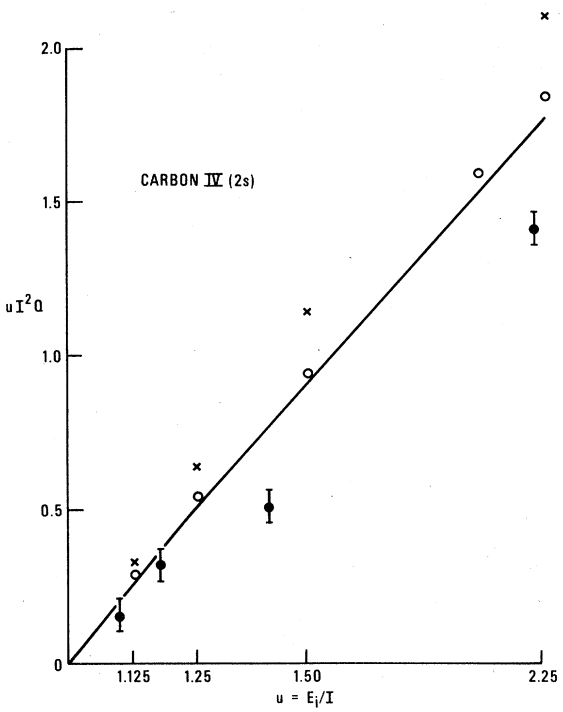

FIG. 5. Fano plot of the scaled electron-impact ionization uI^2Q for C IV(2s) in units of πa_0^2 (Ry)^2. The distorted-wave results were interpolated from Fig. 4. —— DWE (present); • crossed-beam experiment, Ref. 7; ○ Coulomb-Born exchange, Ref. 8; × Coulomb-Born exchange scaled from $Z = \infty$ data, Ref. 9.

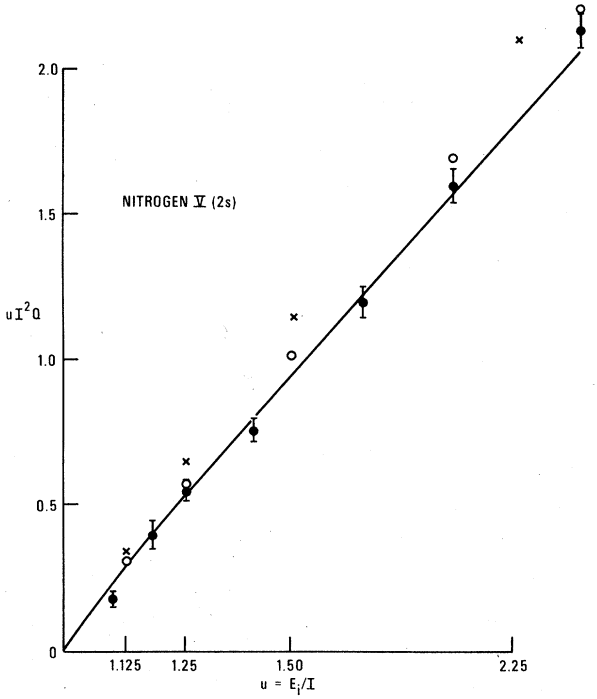

FIG. 6. Fano plot of the scaled electron-impact ionization uI^2Q for N V(2s) in units of πa_0^2 (Ry)^2. The distorted-wave results were interpolated from Fig. 4. —— DWE (present); • crossed-beam experiment, Ref. 7; ○ Coulomb-Born exchange, Ref. 8; × Coulomb-Born exchange scaled from $Z = \infty$ data, Ref. 9.

nonorthogonal orbitals the lithium sequence calculations were repeated using a $2s$ function computed in the same local static potential as the final-state function it overlaps. For Be II, where the effect is largest only a 3% deviation was found.

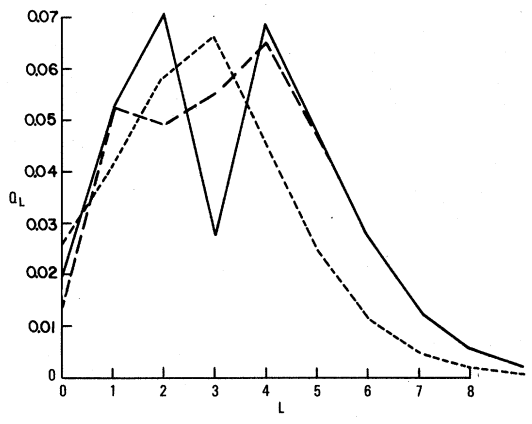

FIG. 7. Partial cross sections for electron-impact ionization of the $2s$ electron of Be II in units of πa_0^2. L is the total angular momentum of the electron plus atom system which, since the ground state is ^2S, is also the orbital angular momentum of the incident partial wave. —— DWT; --- CBT; ----- plane-wave Born.

TABLE V. Partial cross sections $Q(l_e)$ for oxygen 2s ionization. Numbers in parentheses indicate powers of ten, e.g., 0.1234(–5) = 0.1234 × 10^{-5}. Cross sections are in units of πa_0^2.

	$u = 1.125$			$u = 2.25$		
l_e	DWT	CBT	PWB	DWT	CBT	PWB
0	0.5710(–3)	0.5574(–3)	0.1559(–3)	0.1746(–2)	0.1704(–2)	0.1180(–2)
1	0.2956(–3)	0.3035(–3)	0.4123(–4)	0.1905(–2)	0.1920(–2)	0.1157(–2)
2	0.7708(–3)	0.7738(–3)	0.5455(–3)	0.2215(–2)	0.2221(–2)	0.2309(–2)
3	0.6226(–3)	0.6327(–3)	0.3452(–3)	0.2423(–2)	0.2451(–2)	0.2219(–2)
4	0.1171(–3)	0.1147(–3)	0.6864(–4)	0.7027(–3)	0.6961(–3)	0.7314(–3)
5	0.1082(–4)	0.1071(–4)	0.6962(–5)	0.1469(–3)	0.1455(–3)	0.1567(–3)
6	0.6473(–6)	0.6623(–6)	0.4501(–6)	0.2567(–4)	0.2594(–4)	0.2714(–4)
7	0.2352(–7)	0.2404(–7)	0.2117(–7)	0.3571(–5)	0.3630(–5)	0.4034(–5)

The presence of three partial-wave expansions in the electron-impact ionization matrix element makes detailed analysis of angular convergence patterns difficult. Two such convergence patterns, however, were found to be of particular interest. The first, the usual partial cross section Q_L gives the total cross section as a function of the incident angular momentum. Since the targets here are in S states this is also the total orbital momentum of the electron plus ion system. Although the hydrogenic ions all had Q_L spectra with a single maximum and an exponentially decreasing high-l tail, the lithium-like ions exhibited a double maximum, with the intervening minimum depending on the approximation in which the partial waves were com computed. Figure 7 illustrated this behavior for the Be II $u = 1.50$ partial cross section. Such a minimum in the incident partial-wave angular momenta is analogous to the minima occurring in the generalized oscillator strength[10] plotted versus momentum transfer in the Born approximation. A minimum does not occur for the 1s or 2p ionization cross sections[9] since those orbitals have only one node. In this sense the partial cross section Q_L represents a crude momentum transform of the target interaction.

Another partial-cross section series of interest is the ejected angular momentum partial-cross-section series, i.e., the sums of all partial cross sections for each l_e. As l_e increases, the relative overlap between the bound and ejected orbitals decreases as the partial-wave centrigugal barrier moves outward. The l_e partial-cross section series is thus rapidly convergent, with only 5–7 partial waves required in the energy range 1–2.25 threshold units. Table V lists Q_{l_e} for O VI, demonstrating good agreement between DWT and CBT partial l_e cross sections.

The close agreement between the distorted-wave and Coulomb-Born ionization cross sections implies that the long-range Coulomb potential is most important in determining the total cross section for hydrogen- and lithium-like ions. Short-range target potential distortion which affects low l penetrating orbitals has a noticeable effect on the cross section (> 1%) only for low charge states.

Convergence between the CBT and plane-wave Born total cross sections was not observed in the energy range considered. Based on a previous study of Li-like excitation cross sections[11] it is estimated that such convergence may not occur until several tens of threshold units for the higher ions considered here. Note also that it is not true that PWB and CBT *partial* cross sections agree for increasing l. The long-range Coulomb field affects all l—convergence of CBT-PWB cross sections is only expected for high-*energy* collisions.

Although the agreement between the Coulomb-Born and distorted-wave results indicated a certain insensitivity of the total cross section to the approximation for the scattered wave, it does not follow that final-state *correlation* effects, which also modify the final-state scattered and ejected waves, are also small. Mixing of different partials in the final state by correlation could still have significant effects on individual matrix elements. It does not appear possible to estimate the contribution of final-state correlation; an explicit calculation of such effects is now under way.

[1]E. Hinnov, *Proceedings of the NATO Advanced Study Institute*, edited by M. R. C. McDowell (Plenum, New York, 1979).

[2]K. T. Dolder and B. Peart, Rep. Prog. Phys. 39, 693 (1976).

[3]A. Burgess, H. P. Summers, D. M. Cochrane, and R. W. P. McWhirter, Mon. Not. R. Astron. Soc. 179, 275 (1977).

[4]W. Lotz, Z. Phys. 216, 241 (1968).

[5]M. R. H. Rudge and M. J. Seaton, Proc. Phys. Soc.

London 88, 579 (1966).
[6]B. Peart, D. S. Walton, and K. T. Dolder, J. Phys. B 2, 1347 (1969).
[7]D. H. Crandall, R. A. Phaneuf, and D. C. Gregory, Oak Ridge National Laboratory Report No. ORNL/TM-7020, Oak Ridge, Tennessee (unpublished).
[8]H. Jakubowicz and D. L. Moores (unpublished).
[9]L. B. Golden and D. H. Sampson, J. Phys. B 10, 2229 (1977).
[10]Y. K. Kim, M. Inokuti, G. E. Chamberlain, and S. R. Mielczarek, Phys. Rev. Lett. 21, 1146 (1968).
[11]S. M. Younger (unpublished).